SPANDIDOS PUBLICATIONS

Microarray profiling of gene expression patterns in glomerular cells of astaxanthin-treated diabetic mice: A nutrigenomic approach

YUJI NAITO[1], KAZUHIKO UCHIYAMA[2], KATSURA MIZUSHIMA[2], MASAAKI KURODA[2], SATOMI AKAGIRI[2], TOMOHISA TAKAGI[3], OSAMU HANDA[3], SATOSHI KOKURA[3], NORIMASA YOSHIDA[4], HIROSHI ICHIKAWA[5], JIRO TAKAHASHI[6] and TOSHIKAZU YOSHIKAWA[1-3]

[1]Department of Medical Proteomics, [2]Inflammation and Immunology, [3]Department of Biomedical Safety Science, [4]Molecular Gastroenterology and Hepatology, Graduate School of Medical Science, Kyoto Prefectural University of Medicine, Kyoto 602-8566; [5]Department of Food Sciences and Nutritional Health, The Faculty of Human Environment, Kyoto Prefectural University, Kyoto 606-8522; [6]Fuji Chemical Ind., Nakanikawa-gun, Toyama 930-0397, Japan

Received April 17, 2006; Accepted June 14, 2006

Abstract. We have demonstrated that astaxanthin reduces glomerular oxidative stress as well as inhibits the increase in urinary albumin in diabetic db/db mice. The aim of the present study was to determine the gene expression patterns in the glomerular cells of the diabetic mouse kidney, and to investigate the effects of astaxanthin on the expression of these genes using a high-density DNA microarray. The diet administered to the astaxanthin-supplementation group was prepared by mixing a control powder with astaxanthin at a concentration of 0.02%. Glomerular cells were obtained from the kidneys of mice by laser capture microdissection. Preparation of cRNA and target hybridization were performed according to the Affymetrix GeneChip eukaryotic small sample target labeling assay protocol. The gene expression profile was evaluated by the mouse expression set 430A GeneChip. Array data analysis was carried out using Affymetrix GeneChip operating and Ingenuity Pathway analysis software. Comparison between diabetic db/db and non-diabetic db/m mice revealed that 779 probes (3.1%) were significantly affected, i.e. 550 probes were up-regulated, and 229 probes were down-regulated, both at levels of ≥1.5-fold in the diabetic mice. Ingenuity signal analysis of 550 up-regulated probes revealed the mitochondrial oxidative phosphorylation pathway as the most significantly affected caronical pathway. The affected genes were associated with complexes I, III, and IV located on the mitochondrial inner membrane, and the expression levels of these genes were decreased in mice treated with astaxanthin as compared to the levels in the control mice. In addition, the expression of many genes associated with oxidative stress, collagen synthesis, and transforming growth factor-ß signaling was enhanced in the diabetic mice, and this enhancement was slightly inhibited in the astaxanthin-treated mice. In conclusion, this genome-wide nutrigenomics approach provided insight into genes and putative genetic pathways that are thought to be affected by stimulation by high-glucose concentrations. In addition, the present approach may help us gain a better understanding of the genes and pathways involved in the anti-diabetic mechanism of astaxanthin.

Correspondence to: Dr Yuji Naito, Department of Medical Proteomics, Kyoto Prefectural University of Medicine, Kawaramachi-Hirokoji, Kamigyo-ku, Kyoto 602-8566, Japan
E-mail: ynaito@koto.kpu-m.ac.jp

Key words: Astaxanthin, GeneChip, glomerular cells, nutrigenomics, oxidative phosphorylation, oxidative stress

Introduction

It has been postulated that increased oxidative stress by high glucose concentrations in the blood is important in the pathogenesis of diabetic nephropathy. Studies using natural and synthetic antioxidants have provided convincing evidence that glomerular hypertrophy and the accumulation of collagen and transforming growth factor-ß (TGF-ß) due to high glucose concentrations are largely mediated by reactive oxygen species (1-4). Kaneko and colleagues (1) have reported that antioxidant treatment (N-acetyl-L-cysteine, vitamins C and E) can exert beneficial effects on db/db mice, with the preservation of *in vivo* ß-cell function. It has also been reported that antioxidant treatment with vitamin E, probucol, α-lipoic acid, or taurine normalized not only diabetes-induced renal disorders such as albuminuria and glomerular hypertension, but also various types of glomerular pathology (3). It is thought that such studies might provide further insight into therapeutic strategies for treating patients with diabetes mellitus.

Astaxanthin, a common red-colored pigment found in algae, fish, and birds, is a carotenoid that exerts many highly potent pharmacological effects, including antioxidative

activity (5,6). Astaxanthin is reported to be more effective than other antioxidants such as vitamin E and ß-carotene in the prevention of lipid peroxidation in solution and in various biomembrane systems. In 2002, we first reported the potential usefulness of astaxanthin treatment for reducing glucose toxicity using db/db mice, a rodent model of type 2 diabetes (7). The ability of islet cells to secrete insulin was determined by the glucose tolerance test, and this ability was found to be preserved in an astaxanthin-treated group, although a histological study of the pancreas revealed no significant differences in the ß-cell mass between astaxanthin-treated and -untreated db/db mice (7). Using the same model of diabetic mice, we recently demonstrated that astaxanthin treatment significantly ameliorates diabetic nephropathy, which is detemined based on urinary albumin levels and histological findings (8). In addition, it was clearly observed that long-term oral treatment with astaxanthin reduced not only the increased albuminuria otherwise observed in untreated diabetic mice but also ameliorated such an increase in the urinary excretion of 8-hydroxydeoxy-guanosine (8-OHdG) and in 8-OHdG expression in the mesangial cells with little effect on blood glucose levels (8). Furthermore, our data demonstrated that the esterified astaxanthin used in our previous study was effectively absorbed and was transported successfully to the kidneys (8). Taken together, these results suggested that astaxanthin might directly attenuate diabetic oxidative damage, although a slight decrease in blood glucose levels would also be expected to contribute to the attenuation of such oxidative damage.

In patients with diabetic nephropathy as well as in experimental animal models, various molecules associated with oxidative stress, collagen synthesis, and transforming growth factor-ß (TGF-ß) have been reported to play important roles in the onset and aggravation of diabetic nephropathy (9,10). The enhanced expression of these molecules, the abnormal regulation of cell signaling, and the genetic polymorphism of these genes may all contribute to dysregulated cell proliferation and to an enhanced expansion of the extracellular matrix in the renal glomerular region. Many studies on the pathogenesis of diabetic nephropathy have been based on the analysis of the expression of a single molecule, or a relatively limited number of these molecules in diabetic glomerular cells. Recently, DNA microarray techniques have become available that have enabled the characterization of the mRNA expression pattern of a large number of genes simultaneously. In this study, we identified specific gene expression profiles in the renal glomerular cells of diabetic db/db mice, and we investigated the effects of astaxanthin on the expression of these genes using a comprehensive GeneChip system analysis.

Materials and methods

Animals and experimental design. Six-week-old female db/db mice, a rodent model of type 2 diabetes, and their non-diabetic db/m littermates were purchased from the Clea Japan Co. Ltd. (Tokyo, Japan), and kept under controlled conditions with a 12-h light/dark cycle at 21-25˚C. The mice were fed commercial CE-2 (Clea Japan) with free access to water for 1 week to adapt to the new environment. The CE-2 diet contained (g/100g): moisture 8.9, protein 25.4, fat 4.4, fiber 4.1, ash 6.9, carbohydrates 50.3, and sufficient vitamins and minerals to maintain the health of the mice. The mice were divided into three groups as follows: non-diabetic, db/m; diabetic, db/db; and diabetic db/db treated with astaxanthin. Each of the groups contained 3 mice. The diet for the astaxanthin supplementation group was prepared by mixing CE-2 powder with astaxanthin (Fuji Chem. Industry Co. Ltd, Toyama, Japan) at 0.02%. The food intake was measured daily for 6 weeks before dissection. The body weight of the mice was measured every 7 days. Maintenance of the animals and experimental procedures were carried out in accordance with the guidelines of the US National Institutes of Health for the Use of Experimental Animals. The procedures were approved by the Animal Care Committee of the Kyoto Prefectural University of Medicine.

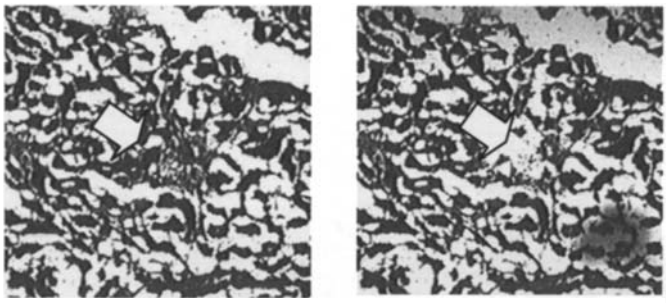

Figure 1. Laser capture microdissection. Renal glomerular cells were isolated by laser-assisted microdissection using an LM200 system. Left, before microdissection; right, after microdissection.

Laser capture microdissection, cRNA amplification, and GeneChip hybridization. We used laser-assisted microdissection to obtain cell-specific RNA. Renal glomerular cells were identified on cryostat sections (8 μm) of specimens obtained from the kidneys of the mice, and the cells were isolated by laser-assisted microdissection using an LM200 system (Olympus, Tokyo, Japan) (Fig. 1). A sample containing several hundred cells was collected from each kidney. Although laser capture microdissection can be used to produce cell-specific RNA, this method is limited by the amount of RNA that can be realistically obtained from captured populations of cells, making it unlikely that the yield would be sufficient for the commonly used GeneChip assay. To overcome this obstacle, our experiments were performed according to the Affymetrix GeneChip Eukaryotic small sample target labeling assay protocol (version II). Using this protocol, we succeeded in obtaining a sufficient amount of biotinylated cRNA to perform the GeneChip analysis from the small amount of renal glomerular cells obtained by laser captured microdissection.

The total RNA was extracted using a Qiagen RNeasy kit (Qiagen, Valencia, CA) and was treated with DNase1 (DNase1 kit, Qiagen) to remove any residual genomic DNA. Briefly, for the first-strand cDNA synthesis, the total RNA sample (1 μl), mixed with T7-Oligo(dT) promoter primer (5 μM, 1 μl), was incubated at 70˚C in a thermal cycler for 6 min, cooled to 4˚C for 2 min, and was reverse-transcribed for 1 h at 42˚C with 3 μl of the RT Premix 1 [1.5 μl DEPC-

ater, 4 μl 5X first-strand buffer, 2 μl DTT (0.1 M), TP mix (10 mM), 1 μl RNase inhibitor (40 U/μl), and 2 μl SuperScript II (200 U/μl)]. The sample was then heated at 70˚C for 10 min to inactivate the SuperScript II, and was cooled to 4˚C. Second-strand cDNA synthesis was carried out by adding 32.5 μl of SS Premix 1 [91 μl DEPC-treated water, 30 μl 5X second strand buffer, 3 μl dNTP mix (10 mM), 1 μl *E. coli* DNA ligase (10 U/μl), 4 μl *E. coli* DNA polymerase I (10 U/μl), and 1 μl RNaseH (2 U/μl)] and incubating the sample for 2 h at 16˚C. The resulting cDNA was treated with 1 μl T4 DNA polymerase (5 U/μl) for 10 min at 16˚C, and was cleaned by ethanol precipitation. To perform *in vitro* transcription, the dried double-stranded cDNA pellet was mixed with the following reagents (10 μl): 4 μl DEPC-treated water, 4 μl premixed NTPs, 1 μl 10X reaction buffer, and 1 μl 10X enzyme mix, and the sample was incubated at 37˚C in a water bath for 6 h. The first-cycle cRNA was cleaned using the RNeasy mini protocol for RNA cleanup accompanying the RNeasy mini kit for cRNA purification (Qiagen, Valencia, CA). For the second cycle of amplification and labeling, the cRNA sample was mixed with random primers (0.2 μg/μl), incubated at 70˚C for 10 min, cooled on ice for 2 min, and incubated at 42˚C for 1 h with 5 μl of the RT Premix 2 [5X first-strand buffer, DTT (0.1 M), dNTP mix (10 mM), RNase inhibitor (40 U/μl), and SuperScript II (200 U/μl)]. Second-strand cDNA synthesis was carried out by mixing the sample with 5 μM T7-Oligo(dT) promoter primer, incubating the resulting mixture at 70˚C for 6 min, cooling it at 4˚C, and re-incubating the sample with 62 μl of SS Premix 2 [43.5 μl DEPC-treated water, 15 μl 5X second strand buffer, 1.5 μl dNTP mix (10 mM), and 2 μl *E. coli* DNA polymerase I (10 U/μl)]. The resulting cDNA was treated with 1 μl T4 DNA polymerase (5 U/μl) for 10 min at 16˚C, and cleaned up by ethanol precipitation. To perform *in vitro* transcription and labeling with the ENZO BioArray high yield RNA transcript labeling kit, the dried double-stranded cDNA pellet was incubated at 37˚C for 4 h with 40 μl of the following reagents: 22 μl DEPC-treated water, 4 μl 10X HY reaction buffer, 4 μl 10X biotin labeled ribonucleotides, 4 μl 10X DTT, 4 μl 10X RNase inhibition mix, and 2 μl 20X T7 RNA polymerase. Labeled cRNA target was cleaned using RNeasy columns. The fragmentation, hybridization, washing, and staining were carried out according to the instructions described in the GeneChip expression analysis technical manual. Affymetrix GeneChip arrays (Affymetrix, Santa Clara, CA) were hybridized with the biotinylated products (5 μg/chip) for 16 h at 45˚C using the manufacturer's hybridization buffer. After washing the arrays, hybridized RNA was detected by staining the sample with streptavidin-phycoerythrin (6X SSPE, 0.01% Tween-20, pH 7.6, 2 mg/ml acetylated bovine serum albumin, and 10 μg/ml of streptavidin-phycoerythrin from Molecular Probes). The DNA chips were scanned using a specially designed confocal scanner (GeneChip Scanner 3000, Affymetrix).

Data analysis. Array data analysis was carried out using Affymetrix GeneChip operating software (GCOS) version 1.0. GCOS analyzes image data and computes an intensity value for each probe cell. Briefly, mismatch probes act as specificity controls that allow the direct subtraction of both background and cross-hybridization signals. To determine the quantitative RNA abundance, the average difference values (i.e., gene expression levels) representing the perfect match-mismatch for each gene-specific probe family was calculated, and the fold changes in average difference values were determined according to Affymetrix algorithms and procedures as follows: I, increase; MI, marginal increase; D, decrease; MD, marginal decrease; and NC, no change. For the pathway analysis, gene probe set ID numbers were imported into the Ingenuity pathway analysis software (Ingenuity Systems, Mountain View, CA). The identified genes were mapped to genetic networks available in the Ingenuity database and were then ranked by a score. The score is the probability that a collection of genes is equal to or greater than the number in a network that could be achieved by chance alone. A score of 3 indicates that there is a 1/1000 chance (p=0.001) that the focus genes randomly occur in a network. Therefore, gene sets with scores of ≥3 have a 99.9% confidence level of not being randomly generated. This score was used as the cut-off for identifying gene networks significantly affected by indomethacin.

Results and Discussion

In the present study, we used a high-density oligonucleotide microarray technique for the mRNA expression profile of renal glomerular cells in order to investigate the mechanism of diabetic nephropathy and to clarify the effects of chronic treatment with astaxanthin on these changes in the levels of mRNA. We used the GeneChip of mouse expression array 430A (Affymetrix), which contained 22,690 probes representing ~15,000 full-length sequences and ~4,000 EST clusters selected from the UniGene database. Comparison of the expression profiles from normal db/m and diabetic db/db mice, and from db/db and astaxanthin-treated db/db mice enabled the identification of differentially regulated genes associated with diabetic-induced hyperglycemia and activity of astaxanthin, respectively.

The present study showed that of the 22,690 probes examined, 779 (3.4%) were up-regulated (550 probes) or down-regulated (229 probes) ≥1.5-fold in the diabetic mice in comparison with the db/m mice (Fig. 2). Tables I and II show ≥5.0-fold up-regulation and down-regulation, respectively, of genes in the diabetic mice in comparison with those of the db/m mice. Among the 550 up-regulated and 229 down-regulated probes in the diabetic mice, the expression levels of 520 (94.5%) and 125 (54.5%) probes, respectively, were reversed by treatment with astaxanthin. To further refine the list of diabetes-affected genes, our next goal was to identify the genes that are known to interact biologically. To this end, we used the pathway analysis tool (Ingenuity System) to carry out analyses of the 550 up-regulated genes. Table III shows 6 genetic networks affected in the glomerular cells of diabetic mice, as defined by the pathway analysis tool. These networks describe functional relationships between gene products based on known interactions reported in the literature. These networks were associated with oxidative phosphorylation, the citrate cycle, ubiquinone biosynthesis, pyruvate metabolism, fatty acid

Table I. Up-regulated genes in db/db mice.

Probe set ID	Descriptions	Average difference[a]		Log ratio	Fold change[b]
		db/db	db/m		
1438634_x_at	LIM and SH3 protein 1	2695.1	10.3	8.0	256.00
1433443_a_at	3-hydroxy-3-methylglutaryl-coenzyme A synthase 1	6472.6	76.6	7.3	157.59
1438610_a_at	Crystallin, ζ	10955.2	95.5	7.1	137.19
1423684_at	---	3573.7	43.8	7.0	128.00
1415820_x_at	---	2286.4	18.0	6.8	111.43
1448382_at	Enoyl-coenzyme A, hydratase/3-hydroxyacyl coenzyme A dehydrogenase	1482.1	27.9	6.7	103.97
1455039_a_at	Transcriptional regulator, SIN3B (yeast)	2383.9	23.7	6.7	103.97
1456176_x_at	DNA segment, Chr 11, ERATO Doi 333, expressed	6941.6	84.7	6.7	103.97
1450387_s_at	---	11485.4	157.3	6.6	97.01
1416180_a_at	Radixin	1363.3	29.0	6.5	90.51
1416633_a_at	RIKEN cDNA 5730536A07 gene	1771.9	14.7	6.5	90.51
1426385_x_at	tyrosine 3-monooxygenase/tryptophan 5-Monooxygenase activation protein, ε polypeptide	3762.1	62.2	6.5	90.51
1437143_a_at	Thioredoxin domain containing 1	7150.4	41.7	6.5	90.51
1455897_x_at	High mobility group nucleosomal binding domain 1	9034.5	77.7	6.5	90.51
1449040_a_at	Selenophosphate synthetase 2	10394.9	103.9	6.4	84.45
1434099_at	---	1091.2	19.6	6.3	78.79
1456196_x_at	---	3454.6	47.8	6.3	78.79
1420037_at	---	6773.1	85.8	6.3	78.79
1449059_a_at	3-oxoacid CoA transferase 1	8173.9	77.6	6.3	78.79
1434499_a_at	Lactate dehydrogenase 2, B chain	9177.8	58.0	6.3	78.79
1424827_a_at	Casein kinase 1, α 1	4755.4	39.8	6.2	73.52
1434892_x_at	Retinoblastoma binding protein 4	7714.7	59.6	6.2	73.52
1423890_x_at	ATPase, Na^+/K^+ transporting, ß 1 polypeptide	76228.2	1190.9	6.2	73.52
1430542_a_at	Solute carrier family 25 (mitochondrial carrier, adenine nucleotide translocator), member 5 phosphoribosylaminoimidazole carboxylase, phosphoribosylaminoribosylaminoimidazole,	3309.2	41.8	6.2	73.52
1436298_x_at	Succinocarboxamide synthetase	2049.5	23.6	6.1	68.59
143544_a_at	Choline phosphotransferase 1	7782.3	153.8	6.1	68.59
1416143_at	ATP synthase, H^+ transporting, mitochondrial FO Complex, subunit F	7867.0	116.2	6.1	68.59
1436900_x_at	Leptin receptor overlapping transcript	1133.7	19.8	6.0	64.00
1427262_at	---	1768.5	46,3	6.0	64.00
1456226_x_at	Discoidin domain receptor family, member 1	5273.1	57.7	6.0	64.00
1436691_x_at	Peroxiredoxin 1	39422.3	367.1	6.0	64.00
1439184_s_at	Thioredoxin-like 5	1615.9	24.4	6.0	64.00
1435791_x_at	Ribosomal protein L17	2858.6	45.3	6.0	64.00
1434056_a_at	Gene model 137, (NCBI)	2872.6	52.0	5.9	59.71
1456341_a_at	Basic transcription element binding protein 1	5894.2	99.7	5.9	59.71
1439411_a_at	Exportin 7	4260.4	40.7	5.9	59.71
1455815_a_at	Tyrosine 3-monooxygenase/tryptophan 5-Monooxygenase activation protein, ß polypeptide	14398.9	205.9	5.9	59.71
1425140_at	Lactamase, ß 2	9634.1	55.9	5.9	59.71
1433514_at	Ethanolamine kinase 1	2752.3	42.6	5.8	55.72
1436783_x_at	Tyrosine 3-monooxygenase/tryptophan 5-Monooxygenase activation protein, ß polypeptide	4090.5	94.2	5.8	55.72
1416316_ at	---	7482.6	104.7	5.8	55.72
1420618_at	Cytoplasmic polyadenylation element binding protein 4	6068.4	55.3	5.8	55.72
1430526_a_at	SWI/SNF related, matrix associated, actin dependent Regulator of chromatin, subfamily a, member 2	1456,4	21.8	5.8	55.72
1426326_at	Zinc finger protein 91	2156.3	39.6	5.7	51.98
1438625_s_ at	Necdin /// PCTAIRE-motif protein kinase 1	2578.6	66.5	5,7	51.98
1420827_a_at	---	2694.3	44.8	5.7	51.98
1433704_s_at	Translocation protein 1	4317.0	112.1	5.7	51.98
1418503_at	Heat shock protein, A	2361.8	22.6	5.7	51.98
1435164_s_at	Ubiquitin-activating enzyme E1C	1787.0	14.3	5.7	51.98
1416166_a_at	Peroxiredoxin 4	557.7	11.3	5.7	51.98

[a]Average difference indicates the level of expression of the gene. [b]Fold changes in average difference values were calculated using an Affymetrix software algorithm (GCOS ver 1.0).

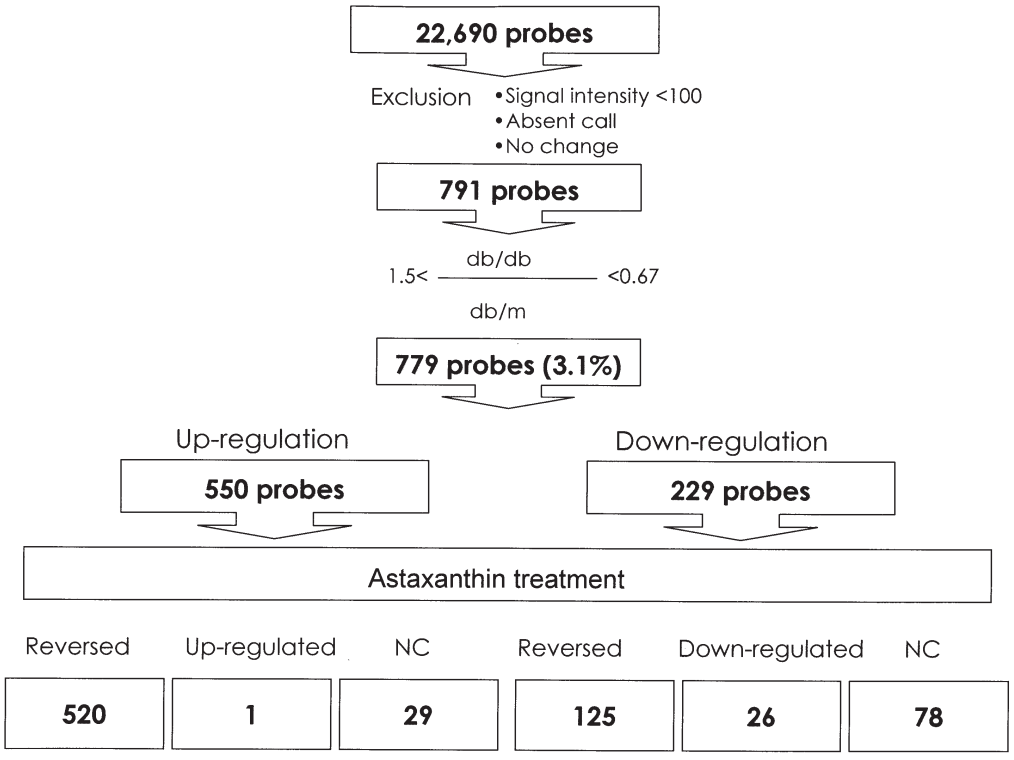

Figure 2. Up- and down-regulated probes in diabetic db/db mice in comparison with db/m mice, and the effect of astaxanthin on the expression of these probes.

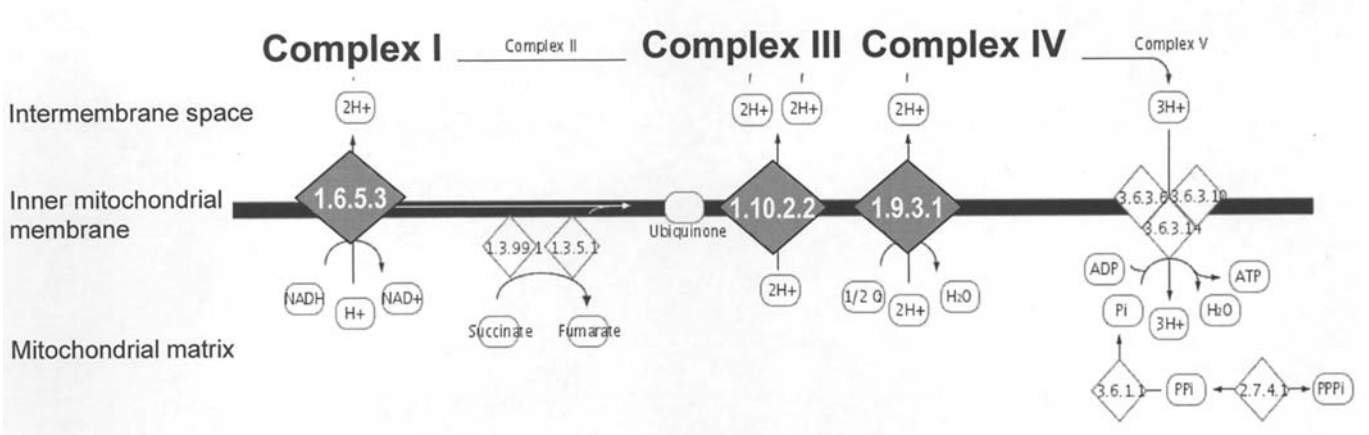

Pathway Node Name	Ingenuity Node Name
1.6.5.3	DAP13, MTND6, NDUFA1, NDUFA2, NDUFA5, NDUFAB1, NDUFB9, NDUFC1, NDUFC2, NDUFS3, NDUFV2
1.10.2.2	UQCRB, UQCRC2
1.9.3.1	COX15, COX5A*, COX5B*, COX6B, COX6C

Figure 3. The oxidative phosphorylation pathway includes 20 sets of probes for genes located at the inner mitochondrial membrane. Descriptions of each probe are provided in Table IV.

Table II. Down-regulated genes in db/db mice.

Probe set ID	Descriptions	Average difference[a]		Log ratio	Fold change[b]
		db/db	db/m		
1452498_at	G patch domain containing 2	11.7	407.6	-5.5	0.02
1421866_at	Nuclear receptor subfamily 3, group C, member 1	18.7	1014.6	-5.4	0.02
1421565_at	Roundabout homolog 3 (*Drosophila*)	51.9	895.8	-5.0	0.03
1420392_at	RIKEN cDNA4930522D07gene	73.2	1150.5	-4.9	0.03
1421380_at	Insulin receptor	21.2	849.6	-4.8	0.04
1427646_a_at	Rho/rac guanine nucleotide exchange factor (GEF) 2	87.6	1978.6	-4.5	0.04
1450193_at	Hyperpolarization-activated, cyclic nucleotide-gated K^+ 1	75.8	1068.3	-4.5	0.04
1420229_at	---	26.1	1305.2	-4.4	0.05
1452129_at	Parathyroid hormone receptor 2	38.3	750.7	-4.3	0.05
1439995_at	Expressed sequence C80638	30.4	1024.0	-4.2	0.05
1451949_at	---	88.6	1114.1	-3.9	0.07
1426042_at	FYVE, RhoGEF and PH domain containing 4	330.2	959.0	-3.9	0.07
1425645_s_at	Cytochrome P450, family 2, subfamily b, polypeptide 10/20	86.6	1301.8	-3.9	0.07
1434079_s_at	Minichromosome maintenance deficient 2 mitotin (*S. cerevisie*)	80.3	996.7	-3.8	0.07
1422117_s_at	KH domain containing, RNA binding, signal transduction Associated 2	137.9	1484.6	-3.8	0.07
1419306_at	RIKEN cDNA 4921513E08 gene	65.3	1141.5	-3.7	0.08
1426870_at	F-box only protein 33	86.6	1660.0	-3.7	0.08
1422926_at	Melanocortin 2 receptor	85.0	1551.0	-3.7	0.08
1449736_at	Phosphatidylinositol-4-phosphate 5-kinase, type II, α	36.3	791.5	-3.6	0.08
1422707_at	Phosphoinositide-3-kinase, catalytic, γ polypeptide	79.8	953.9	-3.5	0.09
1418947_at	NIMA (never in mitosis gene a)-related expressed kinase 3	62.4	1131.7	-3.5	0.09
1442778_at	Expressed sequence AA511254	131.3	1254.4	-3.5	0.09
1416746_at	H2A histone family, member X	208.3	1766.2	-3.5	0.09
1422390_at	Vomeronasal 1 receptor, C5	143.8	1163.1	-3.4	0.09
1426333_a_at	Inhibitor of κB kinase ß	102.3	1011,0	-3.4	0.09
1419483_at	Complement component 3a receptor 1	47.0	752.5	-3.3	0.10
1421338_at	E74-like factor 4 (ets domain transcription factor)	207.4	2074.2	-3.3	0.10
1427889_at	spectrin α 2	201.0	1100.0	-3.3	0.10
1417161_at	DNA segment, Chr 19, ERATO Doi 144, expressed	138.3	1578.0	-3.2	0.11
1434195_at	Protease, serine, 35	162.5	930.1	-3.1	0.12
1421486_at	Early growth response 3	335.1	5852.2	-3.1	0.12
1415756_a_at	SNAP-associated protein	128.0	874.1	-3.1	0.12
1456521_at	---	128.6	1142.5	-3.0	0.13
1439453_x_at	RIKEN cDNA 1500026D 16 gene	30.3	692.0	-2.9	0.13
1438912_at	Hepatoma-derived growth factor, related protein 2	91.1	1898.0	-2.8	0.14
1438825_at	Calmodulin 3	165.6	3263.2	-2.8	0.14
1416888_at	Fas (TNFRSF6)-associated via death domain	418.1	1534.1	-2.8	0.14
1431345_a_at	TATA box binding protein (Tbp)-associated factor, RNA Polymerase I, B	112.8	1110.3	-2.7	0.15
1449563_at	Contactin 1	115.8	1156.2	-2.7	0.15
1426873_s_at	Junction plakoglobin	481.1	4061.8	-2.7	0.15
1450863_a_at	double cortin and calcium/calmodulin-dependent protein Kinase-like 1	309.9	1276.1	-2.7	0.15
1419402_at	Meiosis-specific nuclear structural protein 1	106.8	983.7	-2.7	0.15
1448000_at	Cell division cycle associated 3	371.3	706.2	-2.6	0.16
1422202_at	Thyroid hormone receptor ß	221.5	788.0	-2.6	0.16
1424040_at	cDNA sequence BC019977	428.2	2446.4	-2.6	0.16
1456697_x_at	Cyclin D binding myb-like transcription factor 1	390.7	1712.3	-2.5	0.18
1450319_at	γ-aminobutyric acid (GABA-A) receptor, subunit ß 2	287.8	3465.3	-2.5	0.18
1418132_a_at	DNA segment, Chr 7, Wayne State University 128, expressed	690.7	3617.5	-2.5	0.18
1425276_at	Fibrosin 1	128.6	814.1	-2.4	0.19
1427552_a_at	Glutathione transferase ζ 1 (maleylacetoacetate isomeras	430.8	1036.7	-2.4	0.19

[a]Average difference indicates the level of expression of the gene. [b]Fold changes in average difference values were calculated using an Affymetrix software algorithm (GCOS ver. 1.)

Ingenuity canonical pathway analysis for up-regulated genes in diabetic db/db mice.

Canonical pathway	Significance	Genes
Oxidative phosphorylation	3 93 x 10^{-8}	COX15, COX5A[a], COX5B[a], COX6B, COX6C, DAP13, MTND6, NDUFA1, NDUFA2, NDUFA5, NDUFAB1, NDUFB9, NDUFC1, NDUFC2, NDUFS3, NDUFV2, UQCRB, UQCRC2
Citrate cycle	1.64 x 10^{-6}	ACLY, ATP5G3, CS, FH, IDH1[a], IDH3B, MDH1[a], MDH2, SUCLA2
Ubiquinone biosynthesis	4.07 x 10^{-6}	DAP13, MTND6, NDUFA1, NDUFA2, NDUFA5, NDUFAB1, NDUFB9, NDUFC1, NDUFC2, NDUFS3, NDUFV2
Pyruvate metabolism	2.33 x 10^{-4}	ACAA1, ACAS2L, ACAT1, ADH5, AKR1A1[a], ALDH9A1, GL01, HADHB, LDHB, MDH1[a], MDH2
Fatty acid biosynthesis (path 2)	6.99 x 10^{-4}	ACAA1, ACAT1, EHHADH, HADHB, HADHSC[a]
Synthesis and degradation of ketone bodies	7.57 x 10^{-3}	ACAT1, HMGCS1[a], OXCT[a]

[a]Duplicates. Gene/Protein IDs with multiple identifiers from the input list mapped to a single gene in the Global Molecular Network.

biosynthesis, and the synthesis/degradation of ketone bodies. The results regarding networks associated with the oxidative phosphorylation pathway were found to be highly significant, since a greater number of identified genes were present in this pathway than would be expected by chance. This pathway includes 20 probe sets for genes located at the inner mitochondrial membrane, and these genes are members of the electron transport system complexes I, III, and IV (Fig. 3). The abnormal up-regulation of these genes may be associated with the increased production of reactive oxygen species (ROS) from the mitochondrial membrane, which has also been demonstrated in previous studies. Recently, Nishikawa *et al* (11) showed that the hyperglycemia-induced production of ROS is abrogated by inhibitors of mitochondrial metabolism or by the overexpression of uncoupling protein-1 (UCP-1) or manganese superoxide dismutase (MnSOD). In addition, normalization of mitochondrial ROS production by each of these agents can prevent glucose-induced activation of protein kinase C, the formation of advanced glycation end products, the accumulation of sorbitol, and the activation of nuclear factor kb (NF-kb) in bovine vascular endothelial cells, as well as in cultured human mesangial cells (11,12), all of which are known to be involved in the development of diabetic complications. The present study showed that the expression of up-regulated mitochondrial genes was decreased by treatment with astaxanthin (Table IV). These data may suggest that astaxanthin can reverse the abnormal function of glomerular cell mitochondria in diabetic db/db mice.

Next, in order to focus on diabetic nephropathy, the number of genes was narrowed down to 247 probe sets, which were selected using software of NetAffyx™ analysis center (http://www.affymetrix.com/analysis/index.affx, July 1, 2005) and the following keywords; oxidative stress, transforming growth factor (TGF), and collagen. Among 90 probes related to oxidative stress, 21 were up-regulated in the diabetic db/db mice, as compared to the db/m mice. As shown in Table V, 3 probes of tyrosine 3-monooxygenase were up-regulated at least 8.0-fold in the diabetic mice in comparison with the db/m mice; however, there were no significant differences between the db/db mice and the astaxanthin-treated db/db mice. The peroxiredoxin 1 gene probe (1436691_x_at) was a highly up-regulated gene in diabetic mice and was significantly reduced by a ratio of 0.14 by treatment with astaxanthin. In the mouse expression array 430A (Affymetrix), four probe sets were included for the peroxiredoxin gene: 1436691_x_at, 1433866_x_at, 1434731 _x_at, and 1437014_x_at. The expression of all four probes was up-regulated at least 8.0-fold in the diabetic mice, and was down-regulated by treatment with astaxanthin (Table V). Peroxiredoxin 1 has been shown to play an important role in the defense against oxidative stress (13), and thus the enhanced expression of peroxiredoxin 1 indicates the presence of such stress. Similar to peroxiredoxin 1 expression, the mRNA expression of catalase (1416430_at, 1416429 _a_at), superoxide dismutase 1 (1451124_at), and glutathione peroxidase 3 (1449106_at) was also increased in diabetic mice, and these increases were significantly inhibited by treatment with astaxanthin. Our previous study showed that astaxanthin accumulated in the kidneys of mice after 3 weeks of the administration of a diet containing 0.02% astaxanthin (8). Therefore, the inhibition of the expression of these oxidative stress-responsive genes by an astaxanthin-containing diet, demonstrated in the present study, may indicate that astaxanthin absorbed from the intestine can act as an antioxidant in the glomerular lesion *in vivo*. The present data are also consistent with those of the our previous study, in which urinary and kidney 8-hydroxydeoxyguanosine levels, an index of oxidative DNA damage, exhibited marked reduction by treatment with astaxanthin, in spite of high blood glucose conditions.

It has been demonstrated that the activation of protein kinase C (PKC) and the stimulation of the fibrogenic TGF-ß system by diabetogenic factors such as hyperglycemia and increased protein glycation are pathogenetically linked to the process of diabetic nephropathy (14-16). Diabetic nephropathy is also associated with renal overproduction of the extracellular matrix proteins fibronectin and type IV collagen, as well as with the increased expression of the mRNA encoding these proteins (17,18). The importance of TGF-ß signaling in the

Table IV. Up-regulation of mitochondrial oxidative phosphorylation-related genes and their inhibition by astaxanthin.

Probe set ID	Gene	Descriptions	Complex[a]	Average differerence[a]			Diabetic/normal		Astaxanthin/diabetic	
				Normal db/m)	Diabetic (db/db)	Astaxanthin	Fold change[b]	Change[c]	Fold change[b]	Change[c]
1437982_x_at	COX15	COX15 homolog, cytochrome c oxidase assembly protein (yeast)	I	87.9	1364.1	568.5	8.57	I	0.35	D
1415933_a_at	COX5A	Cytochrome c oxidase, subunit Va	I	319.2	13526.1	1413.6	42.22	I	0.11	D
1439267_x_at	COX5A	Cytochrome c oxidase, subunit Va	I	113.1	3745.5	473.8	27.86	I	0.08	D
1454716_x_at	COX5B	Cytochrome c oxidase, subunit Vb	I	119.8	3289.9	131.3	24.25	I	0.04	D
1456588_x_at	COX5B	Cytochrome c oxidase, subunit Vb	I	455.9	12085.5	971.6	24.25	I	0.11	D
1436757_a_at	COX6B	Cytochrome c oxidase, subunit Vlb polypeptide 1	I	507.4	27966.1	3613.4	24.25	I	0.13	D
1434491_a_at	COX6C	---	I	1544.9	11653.9	2087.8	18.38	I	0.22	D
1455997_a_at	UQCRB	Ubiquinol-cytochrome c reductase binding protein	III	3691.3	67817.7	8314.1	22.63	I	0.13	D
1435757_a_at	UQCRC2	Ubiquinol cytochrome c reductase core protein 2	III	139.7	4108.4	603.3	34.30	I	0.13	D
1455806_x_at	DAP13	RIKEN cDNA 2410011 G03 gene	IV	93.0	1738.4	125.6	13.00	I	0.08	MD
1426088_at	MTND6	---	IV	3578.9	87672.0	12739.6	21.11	I	0.18	D
1422241_a_at	NDUFA1	NADH dehydrogenase (ubiquinone) 1, α subcomplex, 1	IV	1324.9	15002.2	1458.0	9.19	I	0.11	D
1417368_s_at	NDUFA2	NADH dehydrogenase (ubiquinone) 1, α subcomplex, 2	IV	744.8	2544.3	178.8	4.29	I	0.04	MD
1417285_a_at	NDUFA5	NADH dehydrogenase (ubiquinone) 1, α subcomplex, 5	IV	44.7	6785.8	1440.3	36.76	I	0.16	D
1447919_x_at	NDUFAB1	NADH dehydrogenase (ubiquinone) 1, α/ß subcomplex, 1	IV	380.9	3425.9	782.6	12.13	I	0.29	NC
1436803_a_at	NDUFB9	NADH dehydrogenase (ubiquinone) 1, ß subcomplex, 9	IV	226.8	6186.5	1556.8	13.93	I	0.33	NC
1448284_a_at	NDUFC1	NADH dehydrogenase (ubiquinone) 1, subcomplex unknown, 1	IV	214.0	3344.7	848.2	14.93	I	0.27	NC
1455036_s_at	NDUFC2	NADH dehydrogenase (ubiquinone) 1, subcomplex unknown, 2	IV	232.8	24253.0	2846.3	36.76	I	0.14	D
1423737_at	NDUFS3	NADH dehydrogenase (ubiquinone) Fe-S protein 3	IV	94.6	1022.0	277.7	13.93	1	0.12	NC
1452692_a_at	NDUFV2	NADH dehydrogenase (ubiquinone) flavoprotein 2	IV	995.3	3681.2	403.6	3.48	1	0.12	D

[a]Average difference indicates the level of expression of the gene. [b]Fold changes in average difference values were calculated using an Affymetrix software algorithm (GCOS ver. 1.0). [c] I, increase; D, decrease; and NC, no change in the average difference.

pathophysiology of diabetic nephropathy is, in part, confirmed by the results of the present study. Of the 157 probes for genes related to TGF-ß and collagen signaling, 24 were up-regulated in diabetic db/db mice, as compared to db/m mice (Table V). Of the 24 up-regulated probes, the expression of only 5 (transglutaminase 2, guanine nucleotide binding protein, proteasome subunit ß3, ubiquitin B, and secreted phosphoprotein) was significantly decreased by the treatment with astaxanthin, as shown in Table V.

We observed increased expression of two probes of transglutaminase 2 (1433428_x_at, 1437277_x_at) in the db/db mice. It has been reported that tissue transglutaminase enzyme is implicated in protein crosslinking by the formation of increased ε-(γ-glutamyl) lysine bonds between extracellular matrix components in the diabetic kidneys of both db/db mice and human patients with diabetes (19). The present study revealed that this increased expression was markedly reversed by treatment with astaxanthin. These data indicate the possible pathogenic role of transglutaminase 2 in the development of diabetic nephropathy. Furthermore, secreted phosphoprotein 1 is known to be a homolog of human osteopontin. Recent studies have demonstrated that osteopontin plays a role in regulating the accelerated mesangial cell growth and collagen synthesis found in a hyperglycemic environment (20), and it has also been shown that plasma osteopontin is elevated along with the progression of diabetic nephropathy (21). In the present study, a probe of secreted phosphoprotein 1 (1449254_at) was up-regulated at a ratio of 4.92 in diabetic mice, and this effect was significantly inhibited by treatment with astaxanthin at a ratio of 0.13. These findings suggest that secreted phosphoprotein 1 may be a good bio-marker for evaluating the efficacy of dietary food

The effects of astaxanthin treatment on oxidative stress-, cytokine-, TGF-, and collagen-related gene expression.

Probe set ID	Descriptions	Average differerence[a]			Diabetic/normal		Astaxanthin/diabetic	
		Normal db/m)	Diabetic (db/db)	Astaxanthin	Fold change[b]	Change[c]	Fold change[b]	Change[c]
Oxidative stress								
1426385_x_at	Tyrosine 3-monooxygenase/tryptophan 5-monooxygenaseactivation protein, ε polypeptide	62.2	3762.1	1053.6	90.51	I	0.25	NC
1436691_x_at	Peroxiredoxin 1	367.1	39422.3	5075.8	64.00	I	0.14	D
1425993_a_at	Heat shock protein 105	34.5	1804.2	174.5	34.30	I	0.09	NC
1427442_a_at	Amyloid ß (A4) precursor protein	340.3	20915.3	4786.4	34.30	I	0.25	D
1439443_x_at	Transketolase	190.2	7265.6	1082.8	32.00	I	0.14	D
1416430_at	Catalase	53.5	1011.5	360.9	25.99	I	0.33	NC
1419821_s_at	Isocitrate dehydrogenase 1 ($NADP^+$), soluble	118.3	2713.1	1141.9	21.11	I	0.33	NC
1416429_a_at	Catalase	666,3	12753.2	3273.1	18.38	I	0.13	D
1433866_x_at	Peroxiredoxin 1	899.7	8801.4	1255.8	18.38	I	0.18	D
1418180_at	Trans-acting transcription factor 1	73.0	1358.2	527.7	18.38	MI	0.38	NC
1451124_at	Superoxide dismutase 1, soluble	169.9	5222.6	1160.1	17.15	I	0.23	D
1418127_a_at	Programmed cell death 8	130.7	1978.9	1072.6	16.00	I	0.27	D
1434731_x_at	Peroxiredoxin 1	1701.0	19840.5	4196.7	12.13	I	0.11	D
1448808_a_at	Expressed in non-metastatic cells 2, protein	1462.9	9564.2	1215.9	11.31	I	0.13	D
1422433_s_at	Isocitrate dehydrogenase 1 ($NADP^+$), soluble	520.3	7709.1	271.7	10.56	I	0.03	D
1426384_a_at	Tyrosine 3-monooxygenase/tryptophan 5-monooxygenase activation protein, ε polypeptide	63.7	1486.3	592.5	9.85	I	0.25	NC
1438839_a_at	Tyrosine 3-monooxygenase/tryptophan 5-monooxygenase activation protein, ε polypeptide	495.2	3111.5	899.5	8.00	I	0.31	NC
1437014_x_at	Peroxiredoxin 1	507.4	2643.9	600.8	8.00	MI	0.27	D
1449254_at	Secreted phosphoprotein 1	1563.0	5812.8	593.1	4.92	I	0.13	D
1434831_a_at	Forkhead box 03a	514.0	1987.5	116.4	4.29	I	0.05	D
1449106_at	Glutathione peroxidase 3	2488.7	7390.7	1745.1	4.29	MI	0.20	D
Cytokine								
1454610_at	Septin 7	38.9	2514.8	2360.3	48.50	I	0.76	NC
1437457_a_at	Myotrophin	51.1	3157.9	897.4	42.22	I	0.29	MD
1451989_a_at	Microtubule-associated protein, RP/EB family, member 2	142.1	5344.7	966.4	39.40	I	0.23	NC
1434529_x_at	Checkpoint with forkhead and ring finger domains	32.4	805.8	1164.5	32.00	I	1.23	NC
1422486_a_at	MAD homolog 4 (*Drosophila*)	26.4	816.7	934.6	27.86	I	1.00	NC
1448334_a_at	Cyclin I	92.0	3010.4	1323.8	24.25	I	0.47	NC
1416176_at	High mobility group box 1	164.6	2739.8	83.7	22.63	I	0.03	D
1437995_x_at	Septin 7	47.2	1146.4	783.0	22.63	I	0.76	NC
1439405_x_at	RIKEN cDNA 1700051C09 gene	570.9	8937.8	2467.5	22.63	I	0.27	D
1455626_at	Homeo box A9	120.8	2330.3	102.5	22.63	MI	0.04	D
1435324_x_at	High mobility group box 1	59.0	1656.7	454.6	21.11	I	0.31	NC
1425048_a_at	High mobility group box 1	132.9	2033.4	735.2	17.15	I	0.44	MD
1438629_x_at	Granulin	2323.6	26762.6	5119.1	16.00	I	0.19	D
1433540_x_at	Protein phosphatase 1, catalytic subunit, ß isoform	237.0	4846.0	755.6	14.93	I	0.27	D
1439463_x_at	Isomerase	75.0	1434.8	589.2	13.00	MI	0.41	NC
1423792_a_at	Chemokine-like factor super family 6	46.6	1161.3	1603.3	11.31	I	1.23	NC
1420474_at	Myotrophin	582.9	6052.3	1817.3	7.46	I	0.41	NC
1431765_a_at	Ribosomal protein S2	866.9	5207.0	1206.8	6.50	I	0.23	D
MURINE_B2_at	Adenylosuccinate lyase	6470.5	45995.2	19116.6	6.50	I	0.35	NC
1451114_a	Chemokine-like factor super family 6	287.4	1789.7	225.8	5.66	I	0.15	NC
1417606_a_at	Calreticulin	321.4	4176.6	1208.7	4.92	I	0.41	NC
1449254_at	Secreted phosphoprotein 1	1563.0	5812.8	593.1	4.92	I	0.13	D
Collagen								
1456226_x_at	Discoidin domain receptor family, member 1	57.7	5273.1	653.1	64.00	I	0.18	NC
1420811_a_at	Catenin ß	601.6	15719.3	6513.9	32.00	I	0.38	NC
1422486_a_at	MAD homolog 4 (*Drosophila*)	26.4	816.7	934.6	27.86	I	1.00	NC
1435820_x_at	Discoidin domain receptor family, member 1	57.5	1563.4	685.2	24.25	I	0.35	NC
1437277_x_at	Transglutaminase 2, C polypeptide	717.6	11049.1	226.1	11.31	I	0.14	D

Table V. Continued.

Probe set ID	Descriptions	Average differerence[a]			Diabetic/normal		Astaxanthin/diabetic	
		Normal db/m)	Diabetic (db/db)	Astaxanthin	Fold change[b]	Change[c]	Fold change[b]	Change[c]
1433428_x_at	Transglutaminase 2, C polypeptide	175.7	1093.8	149.9	21.11	I	0.08	D
1455900_x_at	Transglutaminase 2, C polypeptide	251.4	3047.0	907.9	19.70	I	0.25	NC
1422555_s_at	Guanine nucleotide binding protein, α 13	55.2	1196.2	120.4	16.00	I	0.16	D
1436991_x_at	Gelsolin	96.4	1207.0	1529.0	16.00	I	0.81	NC
1449334_at	Tissue inhibitor of metalloproteinase 3	341.0	3305.7	1799.2	9.19	I	0.44	NC
1460198_a_at	Proteasome (prosome, macropain) subunit, ß type 3	138.0	2069.9	50.5	8.57	I	0.09	NC
1449436_s_at	Ubiquitin B	5818.2	45009.5	11691.8	8.00	I	0.25	D
1449254_at	Secreted phosphoprotein 1	1563.0	5812.8	593.1	4.92	I	0.13	D
1416953_at	Connective tissue growth factor	1441.9	5698.9	8225.2	4.59	I	1.41	NC
1437628_s_at	Ras homolog gene family, memberA	772.8	3435.1	988.3	4.59	MI	0.31	NC
1426955_at	Procollagen, type XVIII, α 1	90.3	1072.5	57.7	4.29	I	0.09	NC
1425476_at	Procollagen, type IV, α 5	391.2	2292.1	1211.4	4.00	I	0.50	NC
TGF								
1420811_a_at	Catenin ß	601.6	15719.3	6513.9	32.00	I	0.38	NC
1422486_a_at	MAD homolog 4 (*Drosophila*)	26.4	816.7	934.6	27.86	I	1.00	NC
1448184_at	FK506 binding protein 1a	162.0	2046.1	792.5	9.85	I	0.66	NC
1454971_x_at	Transforming growth factor ß 1 induced transcript 4	1093.7	11219.6	3741.1	5.66	I	0.57	NC
1449254_at	Secreted phosphoprotein 1	1563.0	5812.8	593.1	4.92	I	0.13	D
1416953_at	Connective tissue growth factor	1441.9	5698.9	8225.2	4.59	I	1.41	NC
1425742_a_at	Transforming growth factor ß 1 induced transcript 4	1152.8	5321.5	1825.5	4.29	I	0.33	NC

[a]Average difference indicates the level of expression of the gene. [b]Fold changes in average difference values were calculated using an Affymetrix software algorithm (GCOS ver. 1.0). [c]I, increase; MI, marginal increase; D, decrease; MD, marginal decrease; and NC, no change in the average difference.

factors against diabetic nephropathy. In addition, some genes associated with TGF-ß and collagen signaling were up-regulated in the present study, such as connective tissue growth factor (CTGF), TGF-ß 1-induced transcript 4, and type IV procollagen. Although the significant roles played by these genes in the pathogenesis of diabetic nephropathy have been demonstrated, the inhibition of their expression by astaxanthin was not found to to be statistically significant in the present study.

In conclusion, changes in the gene expression profile of glomerular cells in the early phase of diabetic nephropathy in db/db mice were surveyed by laser capture microdissection/GeneChip analysis. In a comparison of db/m and db/db mice, we found that 779 probes showed a ≥1.5-fold difference with respect to the expression levels in each type of mouse. We identified the mitochondrial oxidative phosphorylation pathway as the caronical pathway that is most significantly affected by diabetic nephropathy in mice. Long-term treatment with astaxanthin significantly decreased the expression of up-regulated probes, including those genes associated with oxidative phosphorylation, oxidative stress, and the TGF-ß-collagen synthesis system.

Acknowledgements

This work was supported by a Grant-in-Aid for Scientific Research (15390178 TY) from the Ministry of Education, Culture, Sports, Science and Technology of Japan, and by grants from the Bio-oriented Technology Research Advancement Institution, the Ministry of Agriculture, Forestry and Fisheries of Japan, and from Suzuken Memorial Foundation.

References

1. Kaneto H, Kajimoto Y, Miyagawa J, *et al*: Beneficial effects of antioxidants in diabetes: possible protection of pancreatic beta-cells against glucose toxicity. Diabetes 48: 2398-2406, 1999.
2. Inoguchi T, Tsubouchi H, Etoh T, *et al*: A possible target of antioxidative therapy for diabetic vascular complications-vascular NAD(P)H oxidase. Curr Med Chem 10: 1759-1764, 2003.
3. Koya D, Hayashi K, Kitada M, Kashiwagi A, Kikkawa R and Haneda M: Effects of antioxidants in diabetes-induced oxidative stress in the glomeruli of diabetic rats. J Am Soc Nephrol 14 Suppl 3: S250-253, 2003.
4. Maritim AC, Sanders RA and Watkins JB: Effects of alpha-lipoic acid on biomarkers of oxidative stress in streptozotocin-induced diabetic rats. J Nutr Biochem 14: 288-294, 2003.
5. Naguib YM: Antioxidant activities of astaxanthin and related carotenoids. J Agric Food Chem 48: 1150-1154, 2000.
6. Fukuhara K, Inokami Y, Tokumura A, Terao J and Suzuki A: Rate conctants for quenching singlet oxygen and activities for inhibiting lipid peroxidation of carotenoids and alpha-tocopherol in liposomes. Lipids 33: 751-756, 1998.
7. Uchiyama K, Naito Y, Hasegawa G, Nakamura N, Takahashi J and Yoshikawa T: Astaxanthin protects beta-cells against glucose toxicity in diabetic db/db mice. Redox Rep 7: 290-293, 2002.
8. Naito Y, Uchiyama K, Aoi W, *et al*: Prevention of diabetic nephropathy by treatment with astaxanthin in diabetic db/db mice. BioFactors 20: 49-59, 2004.
9. Connolly SB, Sadlier D, Kieran NE, Doran P and Brady HR: Transcriptome profiling and the pathogenesis of diabetic complications. J Am Soc Nephrol 14: S279-283, 2003.

adel D and van der Woude FJ: Gene expression in
c nephropathy. Curr Diab Rep 4: 462-469, 2004.
11. Nishikawa T, Edelstein D, Du XL, *et al*: Normalizing mitochondrial superoxide production blocks three pathways of hyperglycaemic damage. Nature 404: 787-790, 2000.
12. Kiritoshi S, Nishikawa T, Sonoda K, *et al*: Reactive oxygen species from mitochondria induce cyclooxygenase-2 gene expression in human mesangial cells: potential role in diabetic nephropathy. Diabetes 52: 2570-2577, 2003.
13. Neumann CA, Krause DS, Carman CV, *et al*: Essential role for the peroxiredoxin Prdx1 in erythrocyte antioxidant defence and tumour suppression. Nature 424: 561-565, 2003.
14. Cohen MP, Sharma K, Guo J, Eltayeb BO and Ziyadeh FN: The renal TGF-beta system in the db/db mouse model of diabetic nephropathy. Exp Nephrol 6: 226-233, 1998.
15. Hong SW, Isono M, Chen S, Iglesias-De La Cruz MC, Han DC and Ziyadeh FN: Increased glomerular and tubular expression of transforming growth factor-beta 1, its type II receptor, and activation of the Smad signaling pathway in the db/db mouse. Am J Pathol 158: 1653-1663, 2001.
16. Chen S, Iglesias-de la Cruz MC, Jim B, Hong SW, Isono M and Ziyadeh FN: Reversibility of established diabetic glomerulopathy by anti-TGF-beta antibodies in db/db mice. Biochem Biophys Res Commun 300: 16-22, 2003.
17. Zdunek M, Silbiger S, Lei J and Neugarten J: Protein kinase CK2 mediates TGF-beta1-stimulated type IV collagen gene transcription and its reversal by estradiol. Kidney Int 60: 2097-2108, 2001.
18. Cohen MP, Hud E, Shea E and Shearman CW: Normalizing glycated albumin reduces increased urinary collagen IV and prevents renal insufficiency in diabetic db/db mice. Metabolism 51: 901-905, 2002.
19. El Nahas AM, Abo-Zenah H, Skill NJ, *et al*: Elevated epsilon-(gamma-glutamyl) lysine in human diabetic nephropathy results from increased expression and cellular release of tissue transglutaminase. Nephron Clin Pract 97: c108-117, 2004.
20. Sodhi CP, Phadke SA, Batlle D and Sahai A: Hypoxia and high glucose cause exaggerated mesangial cell growth and collagen synthesis: role of osteopontin. Am J Physiol Renal Physiol 280: F667-674, 2001.
21. Yamaguchi H, Igarashi M, Hirata A, *et al*: Progression of diabetic nephropathy enhances the plasma osteopontin level in type 2 diabetic patients. Endocr J 51: 499-504, 2004.